PHYSICAL REVIEW B VOLUME 22, NUMBER 12 15 DECEMBER 1980

Cluster formation in two-dimensional random walks: Application to photolysis of silver halides

Herbert B. Rosenstock and Charles L. Marquardt
U. S. Naval Research Laboratory, Washington, D. C. 20375
(Received 20 June 1980)

As a model for the growth of silver aggregates on the surface of silver halide crystallites, we have studied the following problem: Independent ions perform random walks on a closed two-dimensional lattice containing, initially, one trap; when a walker reaches a site adjacent to a trap, that site itself becomes a trap. Several simplifications are necessary and justifiable to enable us to use standard random-walk theory: they include replacing the actual crystallite surface by a toroidal one, averaging over all starting points at an early stage, and replacing the irregularly growing cluster by a simply shaped one. Upper and lower limits on the rate of cluster growth are obtained, and results are fitted to experimental observations.

I. INTRODUCTION

The problem we should like to solve is the following: We are given a closed two-dimensional lattice (such as the surface of a small crystal) and particles are performing random walks on it, hopping at prescribed times from the site they are on to a nearest-neighbor site. One of the sites on the lattice differs from the others in being a "trap," which means that when a particle steps onto it, the walk ends, and the site from which the particle stepped onto the trap becomes itself a trap. The number of traps will thus grow as time goes on, depending on the renewed supply of walkers. We want to calculate the speed with which the cluster grows.

The physical motivation for studying this problem is provided by recent experimental work[1-3] which deals with the formation of metallic silver clusters on the surface of silver halide crystallites by ions believed to perform a random walk there. The physical phenomenon is, of course, basic to the photographic process as well of intrinsic physical interest. Also, the general problem of the formation of metallic clusters on a substrate is one of the key issues in the study of catalysis.[4]

The concept of "trapping times" or "first passages"[5,6] is a familiar one in random-walk theory; however, there are sufficient complexities in the present problem to put a complete solution well beyond our reach, even though the solution to several simpler problems is known either explicitly or at least formally. Our aim will therefore be to solve several related but simpler problems and to demonstrate that the problem we are really concerned with is bounded on one side or the other by one of those. We will thus be able to get a good idea of the nature of cluster growth even though we cannot hope to get a direct solution.

One of the "simplifications" that we make almost throughout this paper is the assumption that the walk takes place on a lattice on the surface of a torus rather than the surface of a cube or of a sphere. The reader may wonder why a torus constitutes a simplification over these other surfaces but can be assured that, mathematically, it is for the following reason. In the past, a considerable number of problems, in solid-state physics as well as in random-walk theory,[7,8] have been solved by the use of "cyclic boundary conditions," conditions which in effect amount to replacing a cubic space in n dimensions by an n-dimensional torus. Under ordinary circumstances this is recognized as a flaw which must and, in most cases, can be shown to be of negligible effect. (For example, when the size of the lattice approaches infinity,[9] it is usually easy to show that the "cyclic boundary conditions" do little harm.) Conversely, in these "ordinary" problems it is recognized that the solutions obtained with cyclic boundary conditions do not approximate reality well when the total number of lattice sites is not large. For our problem, we have therefore been able to make a virtue out of this earlier necessity: Results which are valid on toroidal surfaces not only exist and are ready for our use, but they also are likely to be a much better approximation to the closed surfaces we are interested in than results for an infinite open plane would be.

In Sec. II, we will discuss the single trap on a torus, quote the formal expression for trapping times and moments, and evaluate them. We will also average these expressions over the starting points. Section III is somewhat of a digression, establishing a result that greatly simplifies the later calculations: the fact that trapping times are only weakly dependent on the starting points. In Sec. IV the first two mean moments are evaluated explicitly and an effective distribution function is constructed from them. In Sec. V, we consider two additional solvable models (in which traps are located either randomly or along a straight line). Section VI summarizes four solvable models that we have obtained and establishes their relation to

our physical problem; in Sec. VII the most interesting two such models are evaluated in detail and the physical conclusions drawn. Results are summarized in Sec. VIII.

II. A SINGLE TRAP ON A TORUS

We shall study random walks of a particle on a two-dimensional lattice of N^2 sites (N in each direction), with opposite ends identified; that is to say, on two-dimensional toroidal surface. (Generalization to a surface of N_1 by N_2 sites would not be difficult.) For computational purposes, we assume that all sites are alike—no traps are present—but we will soon see that some results will apply directly to a lattice with one trap. We define two related quantities: the probability $f_n(\vec{x})$ that a particle starting at the origin(0, 0) at step 0 will step onto site $\vec{x}=(x_1,x_2)$ for the first time at step n, and the probability $p_n(\vec{x})$ that such a particle will step onto $\vec{x}$ at step n (not necessarily for the first time). The quantity f is the one of importance to our physical problem, for $\sum_n nf_n(\vec{x})$ is equal to the "mean trapping time" on a lattice which has one trap, located at site $\vec{x}$. It is the quantity p, however, which can be calculated more directly.

It is mathematically convenient to define generating functions for f and p:

$$P(\vec{x},s)=\sum_{n=0}^{\infty} s^n p_n(\vec{x})\,, \tag{1}$$

$$F(\vec{x},s)=\sum_{n=1}^{\infty} s^n f_n(\vec{x})\,. \tag{2}$$

(Note the different lower limits.) Once P and F are known, the p and f can be recovered from (1) and (2), but in fact this will not be necessary; F alone will give us the information we need. F and P are found[10] to be related by

$$F(\vec{x},s)=[P(\vec{x},s)-\delta_{\vec{x}\vec{0}}]/P(\vec{0},s) \tag{3}$$

as is shown in Appendix A. P can be obtained by finding the solution to the difference equation

$$p_{n+1}(x_1,x_2)=\tfrac{1}{4}[p_n(x_1+1,x_2)+p_n(x_1-1,x_2)+p_n(x_1,x_2+1)+p_n(x_1,x_2-1)] \tag{4}$$

obeyed by the probabilities p subject to the boundary conditions

$$p_n(x_1+k_1N,x_2+k_2N)=p_n(x_1,x_2) \tag{5}$$

(where k_1, k_2 are integers) which imply that we are working on a toroidal surface, and the initial conditions

$$p_0(\vec{x})=\delta_{x_10}\delta_{x_20} \tag{6}$$

which states that the walk starts at the origin.

The result is[10]

$$P(\vec{x},s)=N^{-2}\sum_{r_1=0}^{N-1}\sum_{r_2=0}^{N-1} e^{2\pi i\vec{r}\cdot\vec{x}/N}/(1-s\lambda) \tag{7}$$

with

$$\lambda=\tfrac{1}{2}(\cos\theta_1+\cos\theta_2)\,,\quad \theta_1=2\pi r_1/N,\quad \theta_2=2\pi r_2/N,\quad \vec{r}=(r_1,r_2)\,; \tag{8}$$

the derivation is indicated in Appendix B.

The fact that $P(\vec{x},s)$ diverges for $s=1$ implies that $\sum p_n$ is infinite—which is expected (because in a finite lattice, any point will eventually be visited an infinite number of times). However, $F(\vec{x},s)=P(\vec{x},s)/P(\vec{0},s)$ must be, and is, finite.

While (7) formally evaluates F [via (3)] as well as P, it does not reveal the functional dependence of the trapping probability f on either time or starting points very transparently. Accordingly, we try to obtain a distribution function, and compute the moments (i.e., the mean values of the powers) of the trapping times as a first step. It is now convenient to redefine $p_n(\vec{x})$ [and $f_n(\vec{x})$] as the probabilities for [first] passage from $\vec{x}$ to $\vec{0}$ at step n (instead of from $\vec{0}$ to $\vec{x}$). On account of the symmetry of our lattice, this is a purely linguistic change with no mathematical consequences.

The kth moment of the trapping time is defined as

$$\mu_k(\vec{x})=\sum_{n=0}^{\infty} n^k f_n(\vec{x})\,. \tag{9}$$

By differentiating (2) with respect to s and then setting s equal to 1 we find

$$\mu_1(\vec{x})=F^{(1)}(\vec{x},1)\,, \tag{10}$$

$$\mu_2(\vec{x})=F^{(2)}(\vec{x},1)+\mu_1(\vec{x})\,, \tag{11}$$

where

$$F^{(k)}(\vec{x},s)=d^kF(\vec{x},s)/ds^k\,.$$

Let us split off the singular part in (7),

$$P(\vec{x},s)=N^{-2}[(1-s)^{-1}+H(\vec{x},s)]\,. \tag{12}$$

where

$$H(\vec{x},s)=\sum_{r_1}\sum_{r_2}{}' e^{2\pi i\vec{r}\cdot\vec{x}/N}/(1-s\lambda)\,, \tag{13}$$

where the prime indicates omission of point (0, 0) from the summation. Then, for any $\vec{x}\neq(0,0)$, (3) can be written

$$F(\vec{x},s)=[1+(1-s)H(\vec{x},s)]/[1+(1-s)H(\vec{0},s)]\,.$$

For s close to unity we can expand the denominator and obtain

$$F(\vec{x},s)=1-(1-s)K(\vec{x},s)+(1-s)^2H(\vec{0},s)K(\vec{x},s)\,,$$

where

$$K(\vec{x},s)=H(\vec{0},s)-H(\vec{x},s)\,. \tag{14}$$

Differentiating this yields the quantities on the right-hand side of (10) and (11), which become

$$\mu_1(\vec{x})=K(\vec{x},1)\,, \tag{15}$$

$$\mu_2(\vec{x})=[\,1+2H(\vec{0},1)]\,K(\vec{x},1)+2\frac{d}{ds}K(\vec{x},s)\Big|_{s=1}\,. \tag{16}$$

We will also need the mean moments $\bar{\mu}_j$ averaged over all starting points $\vec{x}$, $\bar{\mu}_j=N^{-2}\sum_{x_1}\sum_{x_2}\mu_j(\vec{x})$. In Appendix C we find that the averages of the $H(\vec{x},s)$ terms are exactly zero, and only the $H(\vec{0},s)$ terms contribute. We therefore have

$$\bar{\mu}_1=\bar{H}\,, \tag{17}$$

$$\bar{\mu}_2=\bar{H}(1+2\,\bar{H})+2\,\bar{J}\,, \tag{18}$$

with

$$\bar{H}=\sum_r{}'\,1/(1-\lambda)\,,\qquad \bar{J}=\sum_r{}'\,\lambda/(1-\lambda)^2\,. \tag{19}$$

Many of the expressions derived in this section are evaluated by both exact and approximate methods in Appendix D.

III. THE IRRELEVANCE OF STARTING POINTS

This section may seem peripheral to the main trend of the paper, since it provides only a non-quantitative insight into the functional dependence of trapping times. In fact, the result we obtain is essential towards allowing us to proceed further. What we show is that the trapping times do not depend strongly on the distance of the starting point from the trap.

Qualitatively, the essential result appears from the approximate expression (D22) for the first moment (the mean trapping time) derived in Appendix D:

$$\mu_1(\vec{x})=(N^2/\pi)[\ln R^2+\pi] \tag{20}$$

[where we have omitted terms $O(N^{-2})$ in the brackets]. The major qualitative conclusion—that dependence is strong on the linear size N of the lattice (quadratic) but weak on the starting distance R from the origin (logarithmic)—is immediately apparent. This is not only confirmed, but strengthened by Fig. 1 which shows Eq. (20) (solid curve) for fixed $N=50$ as well as some points exactly computed by direct summation of (19). [For example, the point shown at $R=2$ corresponds to starting point $(x_1,x_2)=(2,0)$; that shown at $R=12.72=\sqrt{162}$ to starting point $(x_1,x_2)=(9,9)$.] The first observation is that (20) represents the data quite well except when $|\vec{x}|$ approaches $N/2$, for reasons given at the end of Appendix D. In that region, the true points fall below Eq. (20), making the R dependence even flatter than logarithmic. We thus see that for any given N, $\mu_1(\vec{x})$ will vary only slightly from N^2-1 (as noted in Appendix D): by $(N^2/\pi)\ln(N^2/2)$ at the most.

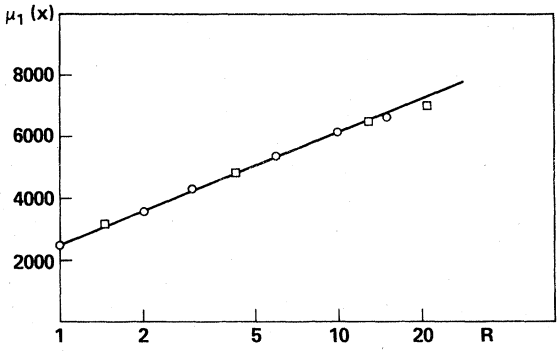

FIG. 1. Mean trapping time versus starting point. The straight line is the approximate analytical expression (20). The points are exact numerical values from direct summation of (19): circles show starting points along the axis ($x_2=0$), squares show starting points along the diagonal ($x_2=x_1$). In both cases, $R=(x_1^2+x_2^2)^{1/2}$. The lattice size is fixed, $N=50$.

The weakness of the x dependence of the trapping time is more convincingly demonstrated by Fig. 2 which shows μ_1 as a function of both starting point and lattice size. The independent variable is N, the linear size of the lattice, and three mean trapping times are plotted: for starting point $(x_1,x_2)=(1,0)$—as close as you can come to the trap, by Eq. (D12) (circles); for starting points $(x_1,x_2)=(N/2,N/2)$—as far away as you can get from the trap, by numerical evaluation of Eq. (15) via (14) and (13) (squares); and the mean for all starting points, Eq. (D18) (solid curve). The closeness of the points for any given N will probably surprise some readers. The "maximum" trapping time is almost indistinguishable from the mean trapping time; the deviation of the minimum trapping time from the mean, small as it is, must be further discounted by noting that on a two-dimensional surface, only few starting points are near the origin (viz., the area element is $2\pi\rho d\rho$, not $2\pi d\rho$). More qualitative discussion appears in Appendix E.

In further work, deviations from the mean will be of the essence: We will, for example, establish a distribution for trapping times. What the work of this section convinces us is allowable is, of course, not to ignore the effect of different starting points entirely, but to average over them be-

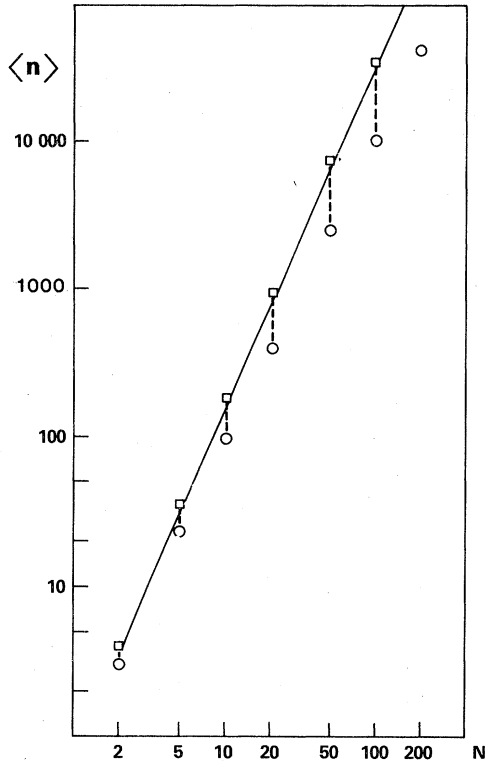

FIG. 2. Average time to trapping for different starting points. Circles: start at (1, 0)—nearest point. Squares: start at $(N/2, N/2)$—most distant point. Solid curve: averaged over all starting points.

fore computing such distributions rather than after. This is fortunate, since otherwise enormous complexity would have to be overcome to make progress.

IV. SINGLE TRAPS: MEAN MOMENTS AND EFFECTIVE DISTRIBUTION

Accordingly, the mean moments, averaged over starting points, as given by (17) and (18) are the only ones we will need. With (D18) and (D19) they become, to sufficient accuracy,

$$\overline{\mu}_1 = (2N^2/\pi)[\ln N + 0.30639], \tag{21}$$

$$\overline{\mu}_2 = (8N^4/\pi^2)[(\ln N)^2 + 0.6126 \ln N + 0.1486] + \frac{2N^2}{\pi}[3 \ln N - 0.4576], \tag{22}$$

Next, we attempt to construct a distribution function $g(t)$ for the trapping time. This may seem overly ambitious since we have only the first two moments (instead of all of them); but we do have additional information—viz., the distribution is 0 at $t=0$, approaches 0 slowly as $t=\infty$, and has a peak in between. It therefore seems plausible to try a linear combination of functions $t^n e^{-ct}$ with $n \geq 1$. This turns out to be impossible because, as shown in Appendix F, for any such function $\overline{\mu}_2/\overline{\mu}_1^2$ is smaller than 2, whereas (21) and (22) require that this ratio be slightly but significantly larger than 2. Now physically, that ratio is the "spread" or variance, properly scaled, of the distribution. Accordingly, we must look for a function with greater variance. The functions $t^n e^{-\sqrt{ct}}$ have that property and are in Appendix F shown to be suitable. The result is

$$g(t) = (\alpha\tau/\xi)(1 + \beta\tau)e^{-\sqrt{\gamma\tau}}, \tag{23}$$

with

$$\tau = t/\xi, \tag{24}$$

$$\xi = N^2 \ln N, \tag{25}$$

$$\alpha = 97.63,$$

$$\beta = 2.6465, \tag{26}$$

$$\gamma = 49.29,$$

a function that is normalized, satisfies (21) and (22), and has all other properties that can reasonably be demanded.

V. TWO ADDITIONAL MODELS

The two models considered in this section are quite different from what is treated in detail in the rest of the paper. This does not signal abandonment of all the work done up till now, but merely our interest, explained in Sec. I, in having different solvable models to compare the situation of interest with.

A. Randomly located traps

We consider briefly a model[11] of randomly located traps on a two-dimensional lattice. While the model is most simply described on an infinite plane, results will also apply to a good approximation to random traps on a torus if the torus is big enough to contain more than just a very few traps. The mean time to absorption is given by

$$\overline{\mu}_1 = \sum_{t=1}^{\infty} tq[V(t) - V(t-1)](1-q)^{V(t-1)}, \tag{27}$$

where q is the density of traps and $V(t)$ the number of distinct sites that would be visited in t steps on a lattice without traps. This quantity is given[10] by

$$V(t) = \pi t/\ln t. \tag{28}$$

See Appendix G for details. (27) can be evaluated by a combination of analytical and numerical methods; the result is shown in Fig. 3 (solid curve). A good analytical approximation to this is given by the individual points shown in Fig. 3, which represent the equation

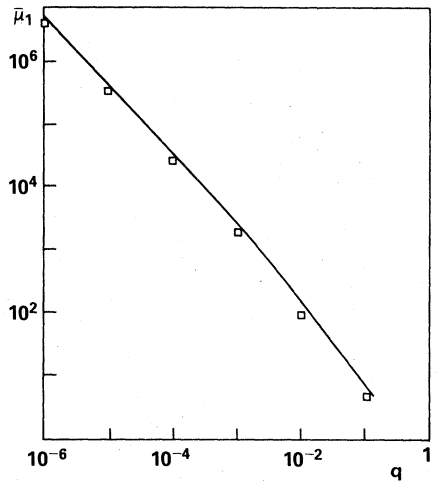

FIG. 3. Trapping times for random traps on a square lattice. See Sec. V A for details.

$$\bar{\mu}_1 = (1/\pi q)[-\ln \pi q + 1 - C] \tag{29}$$

with $C = 0.577\,216$ (Euler's constant).

B. Picket fence

Another useful solvable, though not directly applicable, model is the "picket-fence" model: a line of adjacent traps completely encircling the torus [Fig. 4(a)]. Figure 4 shows, and its caption explains, that this is completely equivalent to infinite strips, a distance N apart, of adjacent traps on a plane. The solution to the latter problem is known[12]; the probability of absorption at step n, averaged over starting points, is

$$p_n = (2/N^2) \sum_{r=1,3,5,\ldots}^{N-1} x^n$$

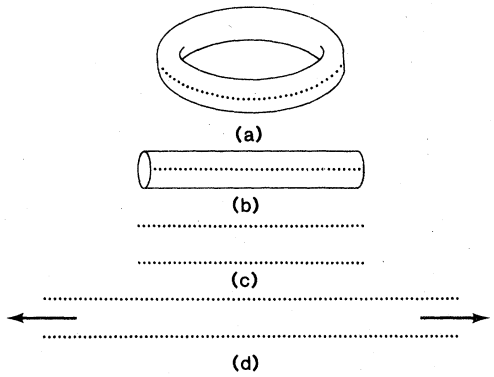

FIG. 4. Picket-fence model: equivalence of two realizations. (a) Line of traps on a torus. (b) Torus has been cut along a meridian, and straightened. (c) Torus has been cut again, along line of traps, and unrolled. (d) Strip extended to infinity to simulate the original periodicity.

with $x = e^{-(\pi r/2N)^2}$. The mean absorption time is therefore

$$\bar{\mu}_1 = \sum_{n=1}^{\infty} n p_n = \frac{2}{N^2} \sum_{r=1,3,5,\ldots}^{\infty} \sum_{n=0}^{\infty} n x^n .$$

The n sum sums to $1/[2\sinh(r^2\alpha)]^2$ where $\alpha = \pi^2/8N^2$ is small; hence only the first few terms in the r sum contribute substantially, and these can be approximated by the first term in their Taylor series:

$$\bar{\mu}_1 = \frac{1}{2N^2}\,\alpha^{-2} \sum_{r=1,3,\ldots} r^{-4} = 0.3332N^2 .$$

VI. SUMMARY OF DIFFERENT MODELS; BRACKETS FOR REALITY

At this point, we have in effect obtained mean trapping times for four situations (and more detail, such as second moments, distribution functions, etc., for some of them). They are worth summarizing.

Model 1. A single trap on a torus, Eq. (21):

$$\bar{\mu}_1 = (2N^2/\pi)[\ln N + 0.306\,39]. \tag{31}$$

The density of traps is $q = 1/N^2$.

Model 2. Randomly located traps on a plane or torus, Eq. (29):

$$\mu_1 = (1/\pi q)[-\ln \pi q + 1 - C]. \tag{32}$$

Model 3. A picket fence of traps:

$$\bar{\mu}_1 = 0.3332N^2. \tag{33}$$

The density of traps is $q = N/N^2 = 1/N$.

Model 4. Periodically repeated traps on an infinite plane (i.e., the traps form a simple cubic lattice on an infinite plane, which is entirely equivalent to a simple cubic lattice on a large torus, and also equivalent to a single trap located on a smaller torus). The formula is quite the same as in model 1, except that we must reinterpret N, the linear size of the real torus, to N', the linear distance between traps:

$$\bar{\mu}_1 = (2N'^2/\pi)[\ln N' + 0.306\,39] \tag{34}$$

with $N' = 1/\sqrt{q}$.

Model 5. This is the label we put on what we are interested in but have not solved: a compact but irregular cluster of traps.

What we can show about model 5 is that it is bracketed in between the others: Model 1 leads to a smaller trapping (and growth) rate, models 2, 3, and 4 to faster ones. The proof for this goes as follows: Consider the 4^j walks of j steps that

would be possible on a "perfect" (i.e., trap-free) lattice, and among them the subset that ends by trapping (i.e., first passage through a trap) at step j. If traps are far apart, or as long as j is smaller than the trap separation, that subset is simply proportional to the trap density, i.e., each trap acts separately, no walk ending at step j at one trap could possibly have passed through another trap earlier. But when the traps are close together, this is no longer true: A walk making a first passage through trap h might have been at trap k earlier and thus terminated earlier. So doubling the number of traps will less than double the number of walks ending at step j. We say that "interference" between traps reduces the amount of trapping, and lengthens the mean duration of the walks. So the question is, given an overal density q of traps, how much interference does each of the five situations above provide?

We argue that model 4 provides the least interference because the traps are as far apart as they can get. Model 2 will provide somewhat more, because with a random arrangement some traps will get close together and tend to interfere more. Model 3 provides a great deal of interference (each trap is interfered with by a neighbor for 2 out of 4 otherwise possible walks), but model 5 provides even more (3 out of 4 walks are interfered with for sites on the surface of the cluster, but for sites in the interior of the clusters, it is worse, viz. 4 out of 4: the "trap" in the interior is wholly inaccessible.) The only model that overestimated the interference is model 1 with all of the traps arbitrarily piled on one site (thus approximating the whole cluster by just one site).

Models 1 and 4 are the ones for which we have the most information, and they provide upper and lower bounds for our physical situations. Accordingly, they are the ones with which we proceed.

VII. SOLUTIONS

A. Model 1

We define $W(t)$ as the number of walkers at time t on an $N\times N$ toroidal surface with one trap. At $t=0$ let $W=W_0$ and at time t, let $A(t)$ walkers be created in the time interval dt. On the other hand, $W_0 g(t)+\int_0^t A(t^*)g(t-t^*)dt^*$ will be lost by trapping, because, according to Sec. IV, walkers created at t^* will be trapped at time t with probability $g(t-t^*)$. Accordingly, W satisfies the differential equation

$$dW=[A(t)-h(t)-W_0 g(t)]dt \tag{35}$$

with

$$h(t)=\int_0^t dt^* A(t^*)g(t-t^*) \tag{36}$$

subject to $W(0)=W_0$. Its solution is

$$W(t)-W_0=\int_0^t dt'[A(t')-W_0 g(t')-h(t')]. \tag{37}$$

We evaluate this for $A(t)=k$, a constant creation rate (though more complicated creation functions would also be tractable). Then

$$W(t)=W_0[1+ct-F_1(t)-cF_2(t)], \tag{38}$$

where

$$c=k/W_0, \tag{39}$$

$$F_1(t)=\int_0^t g(t')dt',$$

$$F_2(t)=\int_0^t F_1(t')dt'. \tag{40}$$

The expressions (41) can be integrated out in closed form, given in Appendix I. The number of walkers at time t if no traps were present would be $W(t)=W_0(1+ct)$; hence the other terms on the right-hand side of (39) are the walkers that have been trapped. On the assumption that each trapped walker becomes itself a trap, the number of traps $V(t)$ is

$$V(t)=1+W_0 F_1(t)+kF_2(t), \tag{41}$$

the first term being the trap that was there to start with. (Note that in this model, lattice size and trap density both remain constant and are simply related by $q=1/N^2$.) Results of evaluation of (42) for various parameters are shown in Fig. 5; see Fig. 7 also.

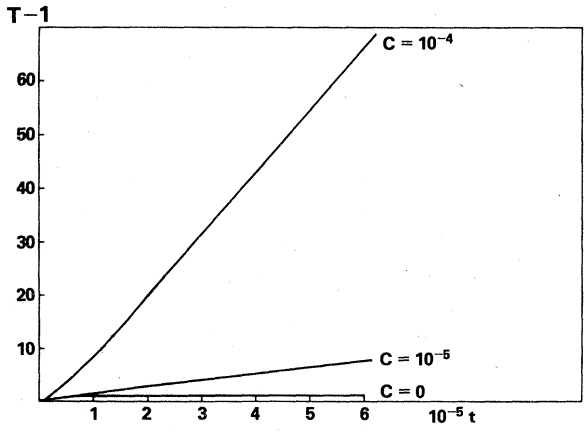

FIG. 5. Model 1. Walkers trapped T versus step number t. c is the number of new walkers created per step. Initially one walker is present. $N=100$.

B. Model 4

In Sec. VII A we calculated the number of walkers trapped by time t. According to our original, physical model of Sec. I, each walker trapped results in the creation of a new trap in the vicinity of the old one; this fact was ignored in Sec. VII A (only at the end, the number of walkers trapped was equated io the number of traps created). Here, we take account of it as we go along.

We do not do so exactly, for the effect of an irregular cluster of traps is not tractable mathematically. Rather, we adhere to the "one trap on a torus" picture, but take account of the increasing trap density by in effect shrinking the torus appropriately whenever a walker is trapped. ("Appropriately" here means simply identifying $1/N^2$ and the trap density q.) As noted in Sec. VI, this will overestimate the effect of the traps (because in this model they are distributed not realistically in a cluster but far away from each other, where they work with the least possible interference from the others); this is good, because in Sec. VII A, their effect was underestimated.

If we start with W_0 walkers and create $k\,dt$ of them as time passes, their total rate of increase will be

$$dW=[k - W_0 g(t) - h(t)]dt\,, \tag{42}$$

where

$$h(t,N(t))=k\int_0^t dt^* g(t-t^*,N(t))$$
$$=k\int_0^t ds\, g(s,N(t))$$

can be evaluated as in Sec. VII A: k walkers are created during dt, but a fraction g of the original ones and a fraction h of the ones created during the walk, are lost by trapping. Since for each walker destroyed, one trap is created, the number V of traps obeys the similar equation

$$dV=[W_0 g(t,N)+h(t,N)]dt\,. \tag{43}$$

We have explicitly indicated that g and h depend on the lattice size N, according to (23) and (39). The crucial step that takes account of the physical effect of the growing cluster size is now to identify N on the right-hand side with $(N_0^2/V)^{1/2}$:

$$dV=[W_0 g(t,N_0/\sqrt{V})+h(t,N_0/\sqrt{V})]dt\,. \tag{44}$$

N_0^2 here is the "original"—that is to say, the actual—number of sites in the lattice. In effect, (45) asserts that the distribution function for V traps among N_0^2 sites can be approximated by that for one trap among N_0^2/V sites. (In Sec. VII A we simply used N_0^2 instead of N_0^2/V.)

This differential equation can now be integrated numerically, step by step, starting with the initial condition $V(0)=1$. Results for various values of the parameters N_0, W_0, and k are shown in Fig. 6.

C. Relation to experiment

Figure 7 shows one experimental growth curve of absorption versus time[2] together with one attempt each to fit it by models 1 and 4 above. We found that model 4 as described above is altogether too efficient in providing an upper limit—a curve chosen to fit experiment at early times soon rises much too rapidly. Accordingly, we replaced the relationship $N^2=N_0^2/V$ by $N^2=N_0^2-V$; this says that the walk on the sites that have not yet become part of the trap cluster can be approximated by one on a square lattice of the same number of total sites. The effect of this change in N is a good deal milder, as might be expected, and fits experiment better, but can no longer be confidently expected to provide an upper limit. The parameters that provide the fit are given in the figure caption. Though the fit is encouraging, these values should be considered preliminary; realistically, for example, one experiment involves crystallites of many sizes, which should be averaged over in the calculation. However, it can be pointed out that certain characteristic features of the experimental curves—e.g., the increasing initial slope followed later by saturation—were not previously reproduced by simpler models; see discussion of Figure 11 in Ref. 2.

Two bits of physical insight may be gained from Fig. 7. Although both model 1 and model 4 give fairly good fits to the growth curve, the parameters required to fit model 1 result in a cluster size which is an order of magnitude smaller than expected from optical measurement, whereas the parameters for model 4 are entirely reasonable.

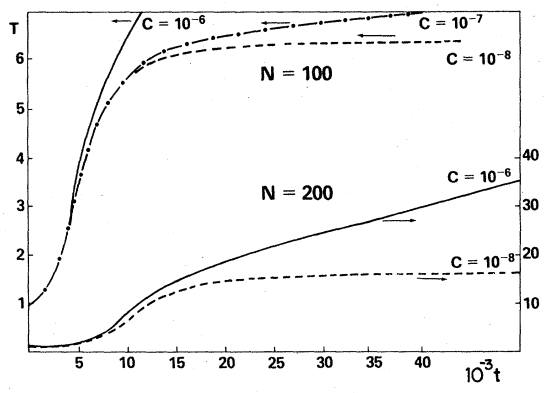

FIG. 6. Model 4. Traps created T versus time t. Parameters as in Figure 5.

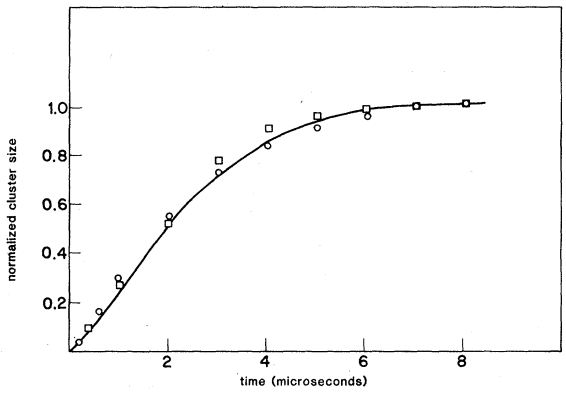

FIG. 7. Curve: growth of absorption (experimental). Squares: Theory, model 1. Lattice of 200 by 200 sites; 108 walkers to start; 4 walkers created per microsecond; 42860 steps per microsecond. Circles: Theory, model 4. Lattice of 200 by 200 sites; 1080 walkers to start; no walkers created later; 47400 steps per microsecond.

This suggests that the shape of the growth curve is determined primarily by the change in trapping cross section of the growing cluster. The source term included in model 1 may be considered as a simplified representation of the diffusion of Ag from the bulk to the surface of the particle. In practice this term would vie with the effect of changing cross section for control of the growth rate. Parameters shown in Fig. 7 (model 1) imply that even in the extreme case where the latter effect is ignored, the diffusion path would account for only a small fraction ($\lesssim 20\%$) of the Ag arriving at the cluster. This appears to be consistent with results obtained by simulating the dependence of growth rate on particle size.[4]

VIII. SUMMARY

We have tried to model a physical situation that has been previously studied experimentally[1-3]: nearly spherical small particles of silver halides become absorbent to visible light within a few microseconds after being irradiated by a short uv pulse. Is is postulated that the pulse produces photoelectrons which combine with Ag ions to form atoms on the surface, that the absorption results from the aggregation of these in a cluster, and that the rate of cluster formation is determined by the random (rather than directed) motion of the Ag on the surface. (It should be noted that the detailed mechanism by which this process occurs is still the subject of considerable debate in photographic science.[13]) We first replaced the (approximately) spherical surface by a toroidal one; this enables us to use and, where necessary extend, the many exact results that exist for random walks on these apparently esoteric surfaces. We went to some trouble to convince the reader that the starting point for the walk does not have much effect on the time it takes to get to the cluster (if one walks randomly it takes a long time, even if one starts nearby) and thus felt justified in averaging over starting points before constructing a distribution function for trapping times rather than after. The feature most resistant to any tractable approximation was the expected irregularity of the growing cluster; several approximations were tried and though lower and upper limits to cluster growth were obtained, the latter is not close enough to reality to be useful. The best fit to experiment was obtained with a model in which the lattice size was decreased as cluster growth removed sites that could be walked on. The final results (Fig. 7) give parameters consistent with some observations; however, observations under different experimental conditions and fits to them must be made before we can be confident of their physical significance.

ACKNOWLEDGMENTS

One of the authors (C. L. M.) wishes to acknowledge helpful discussions with D. A. Nolan, R. J. Araujo and N. F. Borrelli of Corning Glass Co.

APPENDIX A: DERIVATION OF EQUATION (3)

This appendix should clarify the derivation in Ref. 10, which contains several typographical errors. In order to be at point $\vec{x}$ at step n, a walker must have first reached that point at some step $j \leq n$ and then returned to it in $n-j$ steps:

$$p_n(\vec{x}) = \sum_{j=1}^{n} f_j(\vec{x}) p_{n-j}(\vec{0}) .$$

[$p_k(\vec{0})$ was defined as the probability of returning from $\vec{0}$ to $\vec{0}$ in k steps, but because all points in our lattice are equivalent, it is also the probability of return from any point $\vec{x}$ to the same $\vec{x}$.] If we operate on this with $\sum_{n=1}^{\infty} s^n$, the right-hand side becomes, after a little algebra and the use of (1) and (2), $F(\vec{x},s)P(\vec{0},s)$, while the left is $P(\vec{x},s) - p_0(\vec{x},s)$ or, using (6), $P(\vec{x},s) - \delta_{\vec{0}\vec{x}}$. Equating the two yields Eq. (3).

APPENDIX B: ESTABLISHMENT OF $P(\vec{x},s)$, EQUATION (7)

Let us first justify the basic difference equation (4). It says that there are four ways of getting to point $\vec{x}$ at step $n+1$: one must be at one of its four nearest neighbors at step n, and once one is there, the probability of getting to $\vec{x}$ on the next step is $\frac{1}{4}$. Now operate on (4) with $\sum_{n=0}^{\infty} s^n$. On the right-hand side we get $\frac{1}{4}P(x_1+1, x_2, s)$ and three similar terms, and on the left

$$\sum_0 s^n p_{n+1}(\vec{x}) = \frac{1}{s}\sum_0 s^{n+1} p_{n+1} = \frac{1}{s}\left(\sum_0 s^n p_n - p_0\right)$$

which with the use of (1) and (6) becomes $(1/s) \times [P(\vec{x},s) - \delta_{\vec{x}\vec{0}}]$; so (4) becomes

$$P(\vec{x},s) - \tfrac{1}{4}s[P(x_1+1,x_2,s) + P(x_1-1,x_2,s) + P(x_1,x_2+1,s) + P(x_1,x_2-1,s)] = \delta_{\vec{x}\vec{0}} \tag{B1}$$

Performing the same operation on (5) gives

$$P(x_1 + k_1 N, x_2 + k_2 N, s) = P(x_1, x_2, s)\,. \tag{B2}$$

Deducing the solution of (B1) and (B2) is a little involved,[10] but verifying that (7) is in fact a solution is straightforward. (B2) is satisfied because the x's appear in (7) in the exponential only, which are periodic with period kN for any integer k. For (B1), we compute from (7) that

$$P(x_1+1,s) + P(x_1-1,x_2,s) = N^{-2}\sum\sum (e^{2\pi i r_1(x_1+1)} + e^{2\pi i r_1(x_1-1)})e^{2\pi i r_2 x_2}/[1 - \tfrac{1}{2}s(\cos\theta_1 + c\cos\theta_2)]$$

$$= N^2 \sum\sum \frac{2\cos 2\pi r_1 x_1}{1 - (s/2)(\cos\theta_1 + \cos\theta_2)}\, e^{2\pi i \vec{r}\cdot\vec{x}}$$

so that (B1) becomes

$$\sum_{r_1=0}^{N-1}\sum_{r_2=0}^{n-1} e^{2\pi i \vec{r}\cdot\vec{x}} = N^2 \delta_{x_1 0}\delta_{x_2 0}$$

or, separating variables,

$$\sum_{r=0}^{N-1} e^{2\pi i r x} = N\delta_{x0}\,,$$

a representation of the Kronecker delta which many readers will recognize and all can verify. This shows that (7) is indeed the solution of (B1) and (B2), and hence also of (4), (5), and (6).

APPENDIX C: AVERAGE OVER STARTING POINTS

The average of $H(\vec{x},s)$ over starting points is, from (13),

$$\langle H(\vec{x},s)\rangle_{\vec{x}} = N^{-2}\sum_{x_1}\sum_{x_2}\sum_{r_1}\sum_{r_2}{}' \frac{e^{2\pi i \vec{r}\cdot\vec{x}/N}}{(1-s\lambda)}\,.$$

Upon exchanging the order of the $\vec{x}$ and $\vec{r}$ summations, this becomes $N^{-2}\sum_{r_1}\sum_{r_2}'(1-s\lambda)^{-1}F(r_1)F(r_2)$ where $F(r_1)$ is $\sum_{x_1=0}^{N-1} e^{2\pi i r_1 x_1/N}$ and can be summed to give $\delta_{r_1 0}$. But the point $(r_1,r_2)=(0,0)$ is precisely the one which is omitted in the r sums. Therefore $\langle H(\vec{x},s)\rangle_{\vec{x}}$ vanishes.

APPENDIX D: EXPLICIT EXPRESSIONS FOR SECTION II

Here we obtain analytical approximations to $H(\vec{x},s)$ given by (13) and $\bar{J}_1$ its derivative given by (19) in the limit of s close to 1. We do the work separately first for large x (but find that the expression obtained works surprisingly well for small but nonzero x as well); and then for $x=0$.

For nonzero x, we write (13) as

$$H(\vec{x},s) = \sum_{t_1,t_2=-N/2}^{N/2}{}' \frac{e^{i\vec{\theta}\cdot\vec{x}}}{(1-s\lambda)} \tag{D1}$$

with θ given by (8). Use the identity $a^{-1} = \int_0^\infty du\, e^{-au}$ for $a = 1 - s\lambda$, interchange the order of summations and integration, and write

$$s = 1-\epsilon\,, \quad \epsilon = 1 - s\,. \tag{D2}$$

This gives

$$H(\vec{x},s) = \int_0^\infty du\, e^{-\epsilon u} Q(s,\vec{x},u)\,, \tag{D3}$$

where

$$Q(s,\vec{x},u) = \sum_t\sum_t{}' e^{-(1-\epsilon)Fu} e^{i\vec{\theta}\cdot\vec{x}} \tag{D4}$$

with

$$F = 1 - \lambda = f(\theta_1) + f(\theta_2)\,, \quad f(\theta_1) = \tfrac{1}{2}(1-\cos\theta_1)\,.$$

Since the sums are finite ones, no convergence difficulties can arise. In the limit $\epsilon \to 0$ of interest to us, Q becomes independent of ϵ and the sums can be replaced by integrals, yielding

$$Q(1-\epsilon,\vec{x},u) = (N/2\pi)^2 G(x_1,u)G(x_2,u)\,, \tag{D5}$$

where

$$G(x,u) = \int_{-\pi}^{\pi} d\theta\, e^{-uf(\theta)} e^{ix\theta}\,. \tag{D6}$$

Now (D3) can be written as

$$H(\vec{x},s) = \epsilon^{-1}\int_0^\infty dv\, e^{-v} Q(1-\epsilon,\vec{x},v/\epsilon) \tag{D7}$$

and this shows that, when ϵ is small, the last argument $u = v/\epsilon$ of Q will be very large throughout almost all the range of integration. But in that situation, substantial contributions to (D6) can come only from regions where $f(\theta)$ is very small, that is, where θ is close to 0. We can then approximate $f(\theta)$ in (D6) by the first term in its Taylor series and extend the limits to $\pm\infty$. This gives[14]

$$G(x,u) = 2\sqrt{\pi/u}\, e^{-x^2/u}$$

and with (D5)

$$Q(1-\epsilon,\vec{x},u)=(N/2\pi)^2(4\pi/u)e^{-R^2u},$$

where

$$R^2=x_1^2+x_2^2 \tag{D8}$$

is the distance of the starting point from the origin. Thus (D3) becomes

$$H(\vec{x},1-\epsilon)=\frac{N^2}{\pi}\int_0^\infty du\, e^{-\epsilon u}e^{-R^2u}/u$$

which is[15]

$$=(2N^2/\pi)K_0(2R\sqrt{\epsilon}),$$

where the Bessel function $K_0(z)$ is, for small z, given by $-\gamma-\ln(z/2)$ with $\gamma=0.5772157\ldots$, Euler's constant. So finally

$$H(\vec{x},1-\epsilon)=-(N^2/\pi)(\ln\epsilon+2\gamma+\ln R^2). \tag{D9}$$

When $\vec{x}=\vec{0}$ and $s=1$, the expressions for H and its derivative J are given by (19). These look a great deal simpler than (D1); however, the (fortunately excluded) term at the origin becomes infinite and the nearby ones become large; we must therefore be careful when replacing sums by integrals. Our procedure is illustrated in Figs. 8(a)–8(d).

Figure 8(a) shows the "correct" region to be summed over (except for the fact that only two of the four edges should be included—a negligible error since the summand is not large there). In Fig. 8(b) we have replaced the sums by integrals over t, the region about the origin that is to be excluded is shown cross hatched. In Fig. 8(c) the variables of integration are $\theta_j=2\pi t_j/N$. Finally, in Fig. 8(d) we have changed to polar coordinates, $\rho=(\theta_1^2+\theta_2^2)^{1/2}$, $\phi=\arctan\theta_2/\theta_1$. We thus obtain

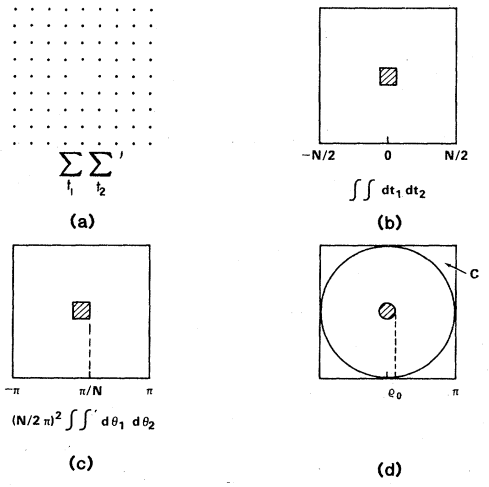

FIG. 8. (a)–(d) illustrate the method of evaluating the expression (19). See text for details.

$$\begin{aligned}(2\pi/N)^2\bar{H}&=A_0+4A_c,\\(2\pi/N)^2\bar{J}&=B_0+4B_c,\end{aligned} \tag{D10}$$

where the first terms are the integrals over the annular ring,

$$\left.\begin{matrix}A_0\\B_0\end{matrix}\right\}=\int_0^{2\pi}d\phi\int_{\rho_0}^{\pi}\rho\,d\rho\times\begin{cases}1/(1-\lambda),\\ \lambda/(1-\lambda)^2,\end{cases} \tag{D11}$$

and the second terms the integral over the "corner" regions C which are shown in Fig. 8(d) and bounded by the circle $\rho=\pi$ and the straight lines $\theta_1=\pi$ and $\theta_2=\pi$,

$$\left.\begin{matrix}A_c\\B_c\end{matrix}\right\}=\int_C\int\rho\,d\rho\,d\phi\times\begin{cases}1/(1-\lambda),\\ \lambda/(1-\lambda)^2.\end{cases} \tag{D12}$$

The major contribution will come from the vicinity of the origin; we therefore evaluate A_0, B_0 by expanding the denominator about the origin and A_c, B_c by replacing the integrand by a constant equal to its average value in the region C.

In doing A_0, B_0 the main question is the proper choice of the radius ρ_0, of the inner circle. A plausible criterion is to make the area of the excluded circle in Fig. 8(d) equal to the area of the excluded square in Fig. 8(c). Since the excluded area in Fig. 8(b) was unity, the excluded area in Fig. 8(c) is $(2\pi/N)^2$, and that in Fig. 8(d) is $\pi\rho_0^2$. Equating these gives $\pi\rho_0^2=(2\pi/N)^2\alpha^2$ where α, a constant of order unity, has been inserted because both the transition from Figs. 8(a) to 8(b), and again from Figs. 8(c) to 8(d), were approximate rather than exact. We therefore chose

$$\rho_0=2\sqrt{\pi}\,\alpha/N. \tag{D13}$$

By expanding the denominator in (D11) we get, to second order in ρ,

$$(1-\lambda)^{-1}=4\rho^{-2}[1+\rho^2 f(\phi)]$$

with (D14)

$$f(\phi)=(\sin^{-4}\phi+\cos^4\phi)/12$$

and (D11) then leads to

$$A_0=8\pi(\ln N-\ln\beta+\ln\pi)+\frac{\pi^3}{4}-\frac{\beta^2\pi}{4N^2}+\cdots,$$

where $\beta=2\sqrt{\pi}\,\alpha$ or, with neglect of terms $O(N^{-2})$ and smaller,

$$A_0=8\pi(\ln N+C'), \tag{D15}$$

where $C'=\ln\pi/\beta+\pi^2/32$ is a constant whose exact value is, like that of β and α, not known at this time. Similarly we obtain

$$B_0=4\alpha^{-2}N^2-4\pi\ln N+D' \tag{D16}$$

with $D'=-16/\pi+4\pi\ln(2\alpha/\sqrt{\pi})$.

Next, we should evaluate A_c and B_c of (D12). However, the reader can see that this result will

be a constant (independent of N) since the integrand is perfectly regular in region C. In (D10) these constants will be added to the expressions (D15) and (D16) which themselves contain undetermined constants. Accordingly, there is no point writing down the values of A_c and B_c; we simply write (D10) as

$$(2\pi/N)^2\bar{H}=8\pi(\ln N+C)\,,$$
$$(2\pi/N)^2\bar{J}=4\alpha^{-2}N^2-4\pi\ln N+D\,, \tag{D17}$$

with $C=C'+(A_c/2\pi)$, $D=D'+B_c$ constants that we can determine by fitting the expression (D17) to (19) as evaluated by direct summation. For $\bar{H}$ this is quite straightforward; evaluate (19) numerically for various N and substitute into (D17). We find that $C=0.3063$ provides an excellent fit, even down to $N=2$ [where we really could not have expected (D17) to be valid]. Even better agreement is obtained if a term in N^{-2} is added,

$$\bar{H}=(2N^2/\pi)[\ln N+0.30639-0.17N^{-2}]\,, \tag{D18}$$

but the fact that the last term is not justified analytically should be kept in mind.

Evaluating the constants in $\bar{J}$ in (D17) is more complicated, since there are two of them, including one which multiplies the leading term. That one is evaluated first, by looking at N large enough to make the others negligible and turns out to be $\alpha^{-2}=0.2193$. We then find that in order to fit the form (D17), the second, logarithmic, term has to be multiplied[16] by -2. We finally obtain

$$\bar{J}=(N/\pi)^2[0.2193N^2+2\pi\ln N-2.4]\,. \tag{D19}$$

It will also be helpful to have an analytical expression for $\mu_1(\vec{x})$ as given by (15) and (14). For this we will need an expression for $H(0,1-\epsilon)$ with ϵ small and positive but not zero, derived in a manner to allow comparison with (D9). From (D1), and with use of (D4), we find

$$H(0,1-\epsilon)=\sum_{t_1}\sum_{t_2}{}'\,1/(\epsilon+F) \tag{D20}$$

to first order in the small quantity F. Proceeding as before via Figs. 8(a)–8(d), we get

$$H(0,1-\epsilon)=\left(\frac{N}{2\pi}\right)^2\int_0^{2\pi}d\phi\int_{\rho_0}^{\pi}\rho\,d\rho/[\epsilon+(\rho/2)^2]\,,$$

where $\rho^2/4$ is the value of F near the lower limit, where most of the contribution to the integral comes from. Upon introducing the variable $\xi=\rho^2/4\epsilon$ this becomes

$$H(0,1-\epsilon)=\left(\frac{N}{2\pi}\right)^2 2\int_0^{2\pi}d\phi\int_{\rho_0/4\epsilon}\frac{d\xi}{1+\xi}$$
$$=(N/2\pi)^2 4\pi\ln[1+(\rho_0^2/4\epsilon)]\,.$$

As $\epsilon\to 0$, this becomes

$$H(0,1-\epsilon)=(N^2/\pi)[-\ln\epsilon+\ln(\rho_0/2)^2]$$

or, with the choice (D13) for ρ_0,

$$H(0,1-\epsilon)(N^2/\pi)[-\ln\epsilon+\ln(\pi/N^2)+\ln\alpha^2]\,.$$

We can combine this with (D9) to get the quantity $K(\vec{x},1-\epsilon)$ defined by(14). As expected, the dependence on ϵ drops out and we find

$$K(\vec{x},1^-)=(N^2/\pi)[\ln R^2+c] \tag{D21}$$

where c is an undetermined constant containing the terms not dependent on $\vec{x}$ or R. It is shown in Appendix H that the expression

$$K(1,0;1)=\mu_1(1,0)=N^2-1 \tag{D22}$$

is exact for all N. Accordingly we write

$$K(\vec{x},1)=\mu_1(\vec{x})=N^2-1+\frac{N^2}{\pi}\ln R^2\,. \tag{D23}$$

From the method of derivation that was used, it is clear that this expression is not valid for all $\vec{x}$ but only for large R (compared to 1), although it also happens to be exact for $\vec{x}=(0,\pm1)$ or $(\pm1,0)$. Furthermore, R must be smaller than $N/\sqrt{2}$, for, as on any other closed surface, you cannot get an unlimited distance away from the origin on a two-dimensional torus. However, the expression agrees surprisingly well with the results of direct evaluation of (14) via (13). The fact that to first order it depends only on the distance R but not the angle ϕ is also of interest.

APPENDIX E: ONE-DIMENSIONAL ANALOG

In one dimension, results analogous to those in Secs. II and III are much simpler and therefore instructive enough to be summarized here even though they have been known for a long time.[18] Consider a cyclic one-dimensional lattice of N sites with one absorber at the origin (or, equivalently, a linear chain of $N+1$ sites with both end sites absorbing). Then the mean duration of a walk starting at site x is[19] $x(N-x)$. This becomes $N-1$ for $x=1$ (starting next to a trap) and $N^2/4$ for $x=N/2$ (starting in the middle, far away from either trap). And averaging over all starting points gives $N(N-1)/6$. This is all the reader needs to know to construct the one-dimensional equivalent of Fig. 2. If he does so, he will find that the spread between the three quantities is much larger than in two dimensions, but still surprisingly narrow; and that walks are unexpectedly long even when starting right next to a trap: On a lattice of 100 sites, that walk will take an average of 99 steps.

APPENDIX F: DISTRIBUTION FUNCTIONS

We need the formula

$$\int_0^\infty e^{-ct}t^n dt = \frac{n!}{c^{n+1}} \tag{F1}$$

It follows that the functions $\psi_n = (c^{n+1}/n!)t^n e^{-ct}$ are normalized; that the quantities

$$m_{jn} = \int_0^\infty t^j \psi_n dt \tag{F2}$$

are given by $(n+j)!/c^j n!$, and that $m_{2n}/(m_{1n})^2 = (n+2)/(n+1)$. This is equal to 2 for $n=0$ but smaller for all $n \geq 1$; the above choice for ψ_n is, therefore, rejected, as explained in Sec. IV.

If we repeat the calculation for

$$\psi_n = [c^{n+1}/2(2n+1)!]t^n e^{-\sqrt{ct}} \tag{F3}$$

(which are also normalized), we instead obtain

$$(m_{2n})/(m_{1n})^2 = (2n+5)(2n+4)/(2n+3)(2n+2)$$

which is larger than 2 for $n=1$ but smaller for $n=2$; with this choice of ψ_n it will, therefore, be possible to find a normalized linear combination

$$g(t) = a\psi_1 + (1-a)\psi_2 \tag{F4}$$

that will satisfy the ratio of moments demanded by (21), (22). To determine the constants a and c, we compute $\mu_1 = \int_0^\infty t\, g\, dt$ and $\mu_2 = \int_0^\infty t^2 g\, dt$ and obtain two equations; upon eliminating c from them, we are left with a quadratic equation in a that has solutions

$$a_\pm = \begin{cases} 1.0798, \\ 0.4822, \end{cases}$$

and corresponding values of

$$c_\pm = (\pi/2N^2 \ln N) \times \begin{cases} 18.25, \\ 31.38. \end{cases}$$

Substituting these into (F4) gives two functions $g_\pm$ which are plotted in Fig. 9(a). We see first, that the two functions are very similar, peaking as expected near $t = N^2$. However, g_+ becomes negative for large enough t [because $1-a$ in (F4) is negative]; this is unacceptable behavior for a distribution function. Accordingly we pick g_- which in its final form is written down in Eqs. (23)–(26).

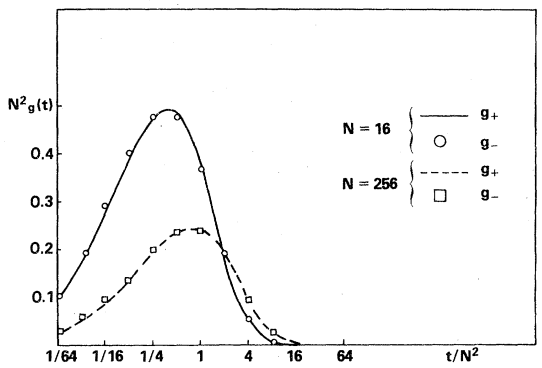

FIG. 9. Distribution functions $g_+(t)$ and $g_-(t)$.

APPENDIX G: DETAILS REGARDING EQUATION (27)

Here we summarize enough of the background to Sec. V to make it appear reasonable; details appear in Ref. 11. There are four parts to Eq. (27). Reading from the right, $(1-q)V^{(t-1)}$ is the probability of not stepping on a trap in the first $t-1$ steps. The bracket is the probability of stepping onto a new site at step t (for an old site would certainly not be a trap), and q is the probability that new site is indeed a trap. Finally $\sum t$ sums the duration t over this probability distribution. To evaluate (27), it is first converted into an integral over V. Then, since the integrand contains t, (28) must be solved for t. This can be done by "Newton's method," an iterative scheme using the initial solution

$$t_0 = (V/\pi)\ln(V/\pi). \tag{G1}$$

The end result of this process is the curve in Figure 3; Equation (29) and the individual points in Figure 3 result from using t_0 of (G1) instead of t.

APPENDIX H: TRAPPING BY NEAREST NEIGHBORS

We evaluate the expression

$$S_D = \sum_{t_1=0}^{N-1} \sum_{t_2=0}^{N-1} \cdots \sum_{t_D=0}{}' (1-\cos\theta_1) \Big/ \left(1 - \frac{1}{D}\sum_{i=1}^{D} \cos\theta_i\right),$$

where $\theta_i = 2\pi t_i/N$ and the prime indicates that the origin is omitted from the summation. S_D is the mean trapping time if the starting point $\vec{x} = (1,0,0,\ldots,0)$ is located next to the trap on a lattice of arbitrary dimension D. Note that S_2 reduces to $K(1,0;1)$, the expression we are really interested in; but keeping D arbitrary here is just as easy, and instructive.

First note that when $t_2, t_3, \ldots, t_D$ are all zero, the summand becomes unity whatever the value of t_1 may be; we can therefore remove the restriction on the summation by writing

$$S_D = -1 + \sum_{t_1=0}^{N-1} \sum_{t_2=0}^{N-1} \cdots \sum_{t_D=0}^{N-1} (1-\cos\theta_1) \Big/ \left(1 - \frac{1}{D}\sum_{i}^{D}(1-\cos\theta)\right)$$

or

$$\frac{1+S_D}{D} = \sum_{t_1=0}^{N-1}(1-\cos\theta_1) \sum_{t_2=0}^{N-1} \cdots \sum_{t_D=0}^{N-1} 1 \Big/ \sum_{i=1}^{D}(1-\cos\theta_i) .$$

Using $a^{-1} = \int_0^\infty e^{-aw} dw$ for the denominator, the variables separate and we can write

$$\frac{1+S_D}{D} = \int_0^\infty du\, J(u) I^{D-1}(u) ,$$

where $I(u) = \sum_{t=0}^{N-1} e^{-u(1-\cos\theta)}$ and $J(u) = \sum_{t=0}^{N-1}(1-\cos\theta)e^{-u(1-\cos\theta)}$. But we see that $J(u) = dI/du$; the integral can therefore be carried out,

$$(1+S_D)/D = (-1/D)[I^D(u)]_0^\infty = [I^D(0) - I^D(\infty)]/D .$$

From the definition of $I(u)$, we see that $I(\infty) = 0$ and $I(0) = N$. Therefore $S_D = N^D - 1$.

APPENDIX I: EXPLICIT EXPRESSIONS FOR SECTION VII A

F_1 and F_2 turn out as follows:

$$F_1(t) = (2\alpha/\gamma^2)[G_3(s) + (\beta/\gamma)G_5(s)] ,$$

$$F_2(t) = (2\alpha/\gamma^2)[U_3(s) + (\beta/\gamma)U_5(s)] ,$$

where

$$U_3(s) = 6t - (2\xi/\gamma)V_3(s) ,$$

$$U_5(s) = 120t - (2\xi/\gamma)V_5(s) ,$$

$$V_j(s) = \sum_{k=0}^{j} a_{jk} G_{j+1}(s) ,$$

and the G_j are given by

$$G_j(s) = j! - H_j(s)e^{-s} ,$$

$$H_0(s) = 1 , \quad H_1(s) = 1 + s , \quad H_j(s) = \sum_{k=0}^{j} a_{jk} s^k ,$$

with

$$a_{j0} = j! , \quad a_{jk} = a_{j,k-1}/k, \ldots, a_{jj} = 1$$

and

$$s = (\gamma t/\xi)^{1/2} .$$

[1] C. L. Marquardt and G. Gliemeroth, J. Appl. Phys. 50, 4584 (1979).

[2] C. L. Marquardt, J. F. Giuliani, and R. T. Williams, J. Appl. Phys. 47, 4915 (1976).

[3] N. F. Borrelli, J. B. Chodak, and G. B. Hares, J. Appl. Phys. 50, 5978 (1979); D. A. Nolan, N. F. Borrelli, and J. W. H. Schreurs, J. Am. Ceram. Soc. 63, 305 (1980).

[4] *Growth and Properties of Metal Clusters: Applications to Catalysis and the Photographic Process*, edited by J. Bourdon (Elsevier, Amsterdam, 1980).

[5] The best general reference for random-walk-theory as used here is W. Feller, *An Introduction to Probability Theory and its Application*, 2nd ed. (Wiley, New York, 1957), Vol. I, Chapters 3, 9, and 14.

[6] See also M. N. Barber and B. W. Ninham, *Random Walks and Restricted Random Walks* (Gordon and Breach, New York, 1970) for a review of some of the detailed papers we cite below.

[7] In solid-state physics, the concept goes back to M. Born and T. von Karman, Phys. Z. 13, 297 (1912).

[8] The applicability of the technique to random-walk problems was probably first recognized by E. W. Montroll, J. Soc. Ind. Appl. Math. 4, 241 (1956).

[9] M. Born, Proc. Phys. Soc. London 54, 362 (1942).

[10] E. W. Montroll and G. H. Weiss, J. Math. Phys. 6, 167 (1965).

[11] H. B. Rosenstock, J. Math. Phys. 21, 1643 (1980).

[12] H. B. Rosenstock J. Soc. Ind. Appl. Math. 9, 169 (1961), Equation (47).

[13] J. F. Hamilton, in *Theory of the Photographic Process*, edited by T. H. James, 4th ed. (MacMillan, New York, 1977), Chap. 4.

[14] H. B. Dwight, *Tables of Integrals and Other Mathematical Data*, 4th ed. (MacMillan, New York, 1961), formula 861.20.

[15] G. E. Roberts and H. Kaufman, *Table of Laplace Transforms* (Saunders, Philadelphia, 1966), p. 17, formula 3.4.

[16] We are not sure why this is. We suspect the truncation implied in going from Fig. 8(a) to 8(b): instead of simply approximating the sum by an integral, a two-dimensional analog of the Euler-MacLaurin formula (Ref. 17) should be used for greater precision. In any case, the $\ln N$ term does not enter our further calculations explicitly.

[17] H. B. Rosenstock, J. Math. Phys. 43, 342 (1964).

[18] Mathematically, the one-dimensional random walk with traps is equivalent to the classical "gambler's ruin" problem.

[19] *An Introduction to Probability Theory and its Application*, Ref. 5, Sec. XIV.3.